Experimental study of stochastic processes for adaptive tilt correction of the signal beam at a long atmospheric path

Arkadiy V. Blank, Vitaliy V. Kapranov, Ruslan V. Mikhailov, Natalia A. Suhareva, Vjatcheslav Yu. Tugaenko

BlankArkadiy@physics.msu.ru

Abstract

The results of experimental study of adaptive correction dynamics for collimated coherence beam at the exit of 1350 meter atmospheric path are presented. The method of phase portraits and chaotic maps for processing the experimental series is used that allowing to visualize the transition phenomenon and the bistable system conditions. The system response to variations of a proportional algorithm parameters for adaptive correction, the frequency of sampling and a scale feedback factor are in details analyzed. Relations of the size of a beam spot on a recording device matrix and the stability of a correction algorithm are experimentally considered.

Introduction

The peculiarity of corrective procedures for laser beams propagating over near-the-ground tilt path is associated with the dynamic and statistical spatial inhomogeneity and non-stationarity of the refractive effects on the beam [1]. Usually available for actuators range of correction frequencies over such paths overlaps only the low-frequency part of the refraction modulation band of the beam displacement vector in the registration plane. Under this mode, effectiveness of the impact should increase when connecting a feedback loop output possessing a sufficient depth of memory.
The dynamical system evolution can be observed in the state space of the system, the modes available can be obtained from the phase portrait as a set of trajectories realized in phase space. Among the trajectories one can mark out a number of basic ones determining the qualitative properties of the system. These include the equilibrium points corresponding to stationary modes of the system and closed trajectories (limit cycles) corresponding to quasi-periodic modes. The stability of a particular mode manifests itself in the consistent behavior of neighboring trajectories, - stable equilibrium or limit cycle attracts all nearby trajectories, unstable ones repels at least some trajectories. The phase portrait, disassembled into groups of

trajectories, allows to describe all types of permissible movements arising under different initial conditions. Actually,the phase portraits apparatus for the description of the dynamics of complex non-stationary systems allows to visualize the solutions of differential or difference equations of a physical system motion [2].

1 The method of phase trajectories

For a system having N degrees of freedom one can map the feasible set of phase trajectories in the 2N вГЎ dimensional phase space. The unit vectors of phase space, in general, correspond to the function and its derivatives with respect to time. Due to uniqueness of differential equations solutions with the necessary set of initial conditions the phase trajectories in the space of correct dimension do not intersect [2]. Crossing of the paths on the reconstructions of phase portraits shows forced reduction of dimension, for example, when using the method of main components. Thus, based on the one-dimensional time sampling and its analysis, one can get a complete picture of a system behavior, combining the dynamic regularities and the statistical characteristics.

The reconstruction procedure of phase trajectories and attractors is based on TakensвГЄ theorem. It is formulated for the embeddings of compact and closed sets [3, 4, 5]. Let A be a compact subset of the G-dimensional space X. Define the embedding subset A in m-dimensional space Y as a transformation of X to Y .The coincidence of two images of the elements, belonging to A, is possible only in case of equality of these elements. According to TakensвГЄ theorem, any smooth transformation X into Y will set the embedding A to Y space on the condition:

$$m \geqslant 2D_A + 1, \tag{1}$$

here D_A вГЎ is a fractal dimension of a set A. For sufficiently large experimental samples the phase trajectories reconstructed from the time series will have the same dimension and mathematical properties as the original physical system.

The experimental 1350 m slant path with small tilt was arranged in the industrial area. [6, 7].A collimated single-mode Gaussian beam of continuous radiation was used. Its power does not exceed 4 Watt. Registration of the intensity distribution at the path output is carried out under the conditions of primary control of spacial beam modulation, at a frame rate of not less than 1 kHz, the sampling frame size is 128x128 pixels, 8-bit width and 1 pt/mm scale. The vector of the first space moments and the corresponding vector of the tilt angles for each video frame will be defined by the discrete intensity distribution:

$$r_x[k] = \frac{\sum_{c=1,128}\sum_{r=1,128} cI(c,r)[k]}{\sum_{c=1,128}\sum_{r=1,128} I(c,r)[k]},\ r_y[k] = \frac{\sum_{c=1,128}\sum_{r=1,128} rI(c,r)[k]}{\sum_{c=1,128}\sum_{r=1,128} I(c,r)[k]}, \tag{2}$$

here r, c - is the number of rows and columns of video selection elements,$I(c,r)[k]$ - is the intensity distribution matrix for the k-th frame of the video sample.

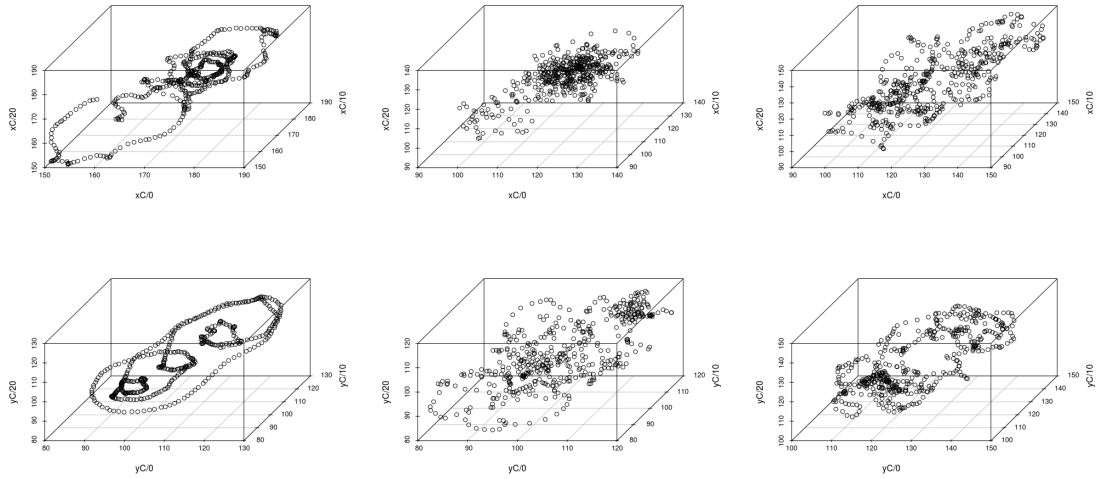

$\beta^2 = 0.3$ $\beta^2 = 1.0$ $\beta^2 = 2.6$

Figure 1: Phase trajectories for X (top) and Y (bottom) component of the first space moment.

The family of phase trajectories one can construct on the base of one dimensional equidistant in time sample by creating the two-dimensional and three-dimensional vectors with a variable time delay between the vector components:

$$(R[i], R[i-d])\,, \ \vec{R}^{(3)}[i] = (R[i], R[i-d], R[i-2d])\,. \tag{3}$$

The phase trajectory profile depends on the ratio of the analyzed system eigenfrequencies and the sampling step. If the ratio вΓЎ $\tau s\omega_i = \pi/2$ (where τ вΓЎ is a sampling step, ω_i вΓЎ is one of the eigenfrequencies) is satisfied, the phase trajectory profile may be close to an ellipse. The optimum value of the delay interval one can select from additional conditions. For example, using the first minimum of the autocorrelation function of the analyzed time series or position of a local minimum of mutual information. According to a given length of the experimental sample N one can get $N - d(m-1)$ vectors, having the coordinates the set of which forms a phase trajectory [8, 9].
Examples of 3D phase portraits for three different turbulence modes characterized by three different values of Rytov parameter are shown in Fig.1. For all six reconstructions the time delay is equal to 10 ms, the coordinates of the vector components are given in millimeters. Note a significant topology difference for horizontal and vertical projections, well conspicuous eigenfrequency components for weakly developed turbulence, the beam characteristics transformation to dynamic chaos mode for moderate turbulence and the emergence of a coherent turbulence at the highest possible values of Rytov number (from those observed in the experiment). In a number of tasks the time scans of 2D phase trajectories can be informative, they allow to estimate the time spent by the system in a specified phase volume, to construct the movement approximations near the singular points of the phase trajectories.

2 Adaptive correction under random noise

Adaptive systems for the correcting of laser beams tilts are well developed for different applied problems, including the electromagnetic propagation through the atmospheric path of various lengths [10, 11]. The main criterion for the effectiveness of system performance leans on the statistics and the misalignment dynamics of the beam orientation and the working system axis. The elaboration of the adaptive correction algorithm, even in the simplest proportional version, demands the control of the beam profile, sample rate of the displacement sensors and the feedback coefficient in the process equation. At the first step of the experimental analysis let us replace the readings of a finite number of sensors of beam shift by a complete set of the meanings of intensity distribution matrix. Let's establish two variable parameter of the adaptive algorithm and one parameter for the beam size. The beam diameter will be varied in the range from 24 mm to 80 mm, by rearranging of the optical parameters of the collimating system.
The experimental results described were obtained under the conditions of a slightly perturbed atmosphere, Rytov parameter does not exceed 1.0 [7]. Sample rate of the displacements sensor varied in the range from 10 Hz to 100 Hz with steps 10 Hz, the feedback coefficient in the adaptive channel varied within $[0.1, 2]$. Here the unit coefficient corresponds to the total compensation of the recorded shift of the beam center for one positioning cycle. Let us represent the discrete equation for the vector projections $\vec{R} = (R_x, R_y)$ of the beam energetic center as follows:

$$\frac{R_i[n+1] - R_i[n]}{\Delta} = \frac{4}{S}(R_{0i} - R_i[n]) + N_i[n], \tag{4}$$

here Δ - is the sampling step, R_{0i} - are the coordinates of the target point on the registration plane, S вГУ is the pre-calibrated scale factor of an adaptive response, N_i вГУ is the anisotropic refractive component of the noise . The initial beam position for all video samples was located in the upper right corner of the working field, at the point with coordinates $(128, 1)$, the target coordinate corresponded to the value $(64, 64)$.

2.1 Variation of the scale correction coefficient

Let's analyze the change in structure of 2D phase trajectories for the fixed sampling rate of the displacements sensors equal to 30 Hz and the optimal beam grouping into a spot of 28 mm diameter. Fig.2 and Fig.3 demonstrate the results of experimental samples processing (scale factor is ranging from 2 -excessive response, to 28 - weak response). A significant difference in the phase portraits for horizontal and vertical correction directions was observed even for the simplest adaptive correction algorithm. For the chosen sampling rate and the compact beam grouping in the recording plane, the phase portraits for X-component demonstrate typical for the proportional algorithm self-oscillating mode under a small correction step and the static displacement in the case of large correction step [10, 11]. For the Y-component, the self-oscillatory mode for chosen sampling rate and the beam profile practically is not observed. The presented phase trajectories for the horizontal

component, show that the chosen range of the response step variations allows to investigate all three operating modes of the adaptive algorithm: self-oscillatory one in the range of the response step $S \subset [2, 8]$, quasiregular mode $S \subset [10, 20]$ and static displacement mode $S \subset [22, 28]$.

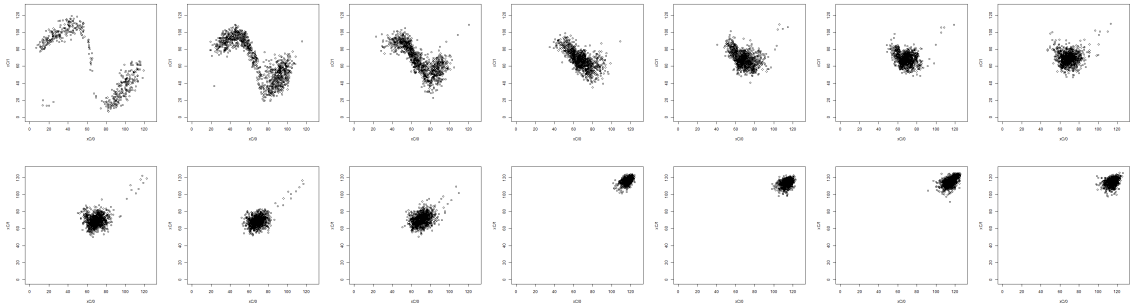

Figure 2: Phase trajectories for the horizontal direction of correction (a response step changes from 2 to 24)

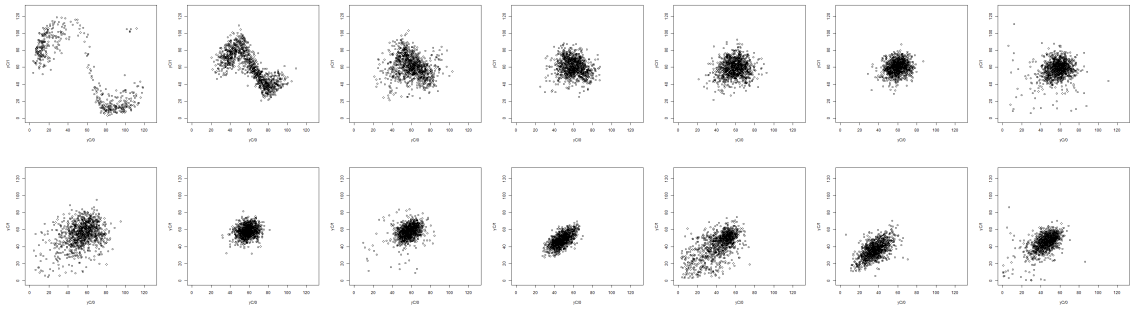

Figure 3: Phase trajectories for the vertical direction of correction (a response step changes from 2 to 24)

2.2 Variation of the sampling time

A random non stationary process in optical density variation of the atmosphere obtains a set of eigenfrequencies defined by both – the turbulent flows and acoustic industrial noise. Their interference spectrum can be determined using methods of nonlinear time-frequency analysis of one-dimensional time series for the components of the vector of the wave beam center, or deriving the spectrum of Poincare recurrence times for the beam phase trajectory (without adaptive correction).
Fig.4 and Fig.5 show the phase trajectories for the horizontal and vertical displacement components in the rate range from 10 Hz to 100 Hz with steps of 10 Hz. The beam grouping is chosen to be the same as for the analysis of the response to the variation of the scale correction coefficient - 28 mm in diameter, the correction scale is equal to 6. The frequency increases from left to right and from top to bottom. A characteristic feature of the observed phase portraits can be considered as the alternation of the regular auto-oscillatory and the unstable chaotic modes for the

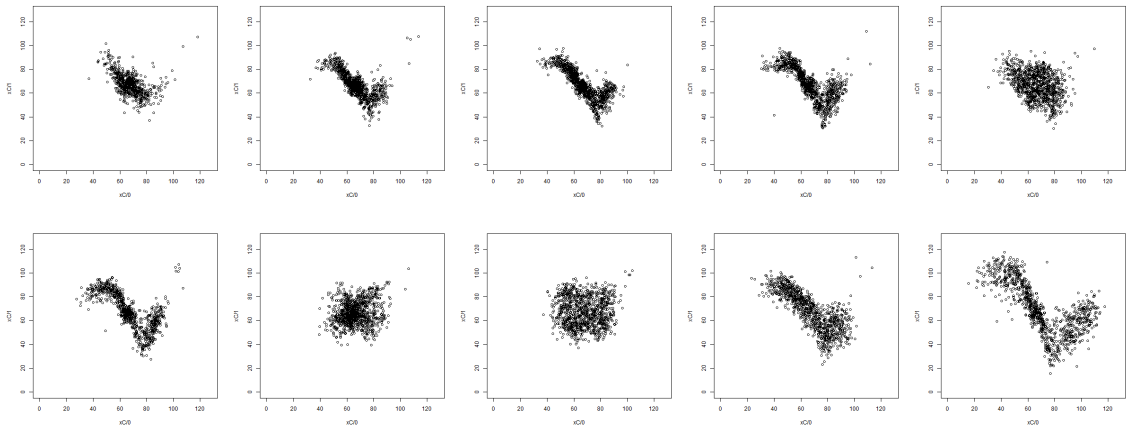

Figure 4: Phase trajectories for X with a frequency rate from 10 Hz to 100 Hz

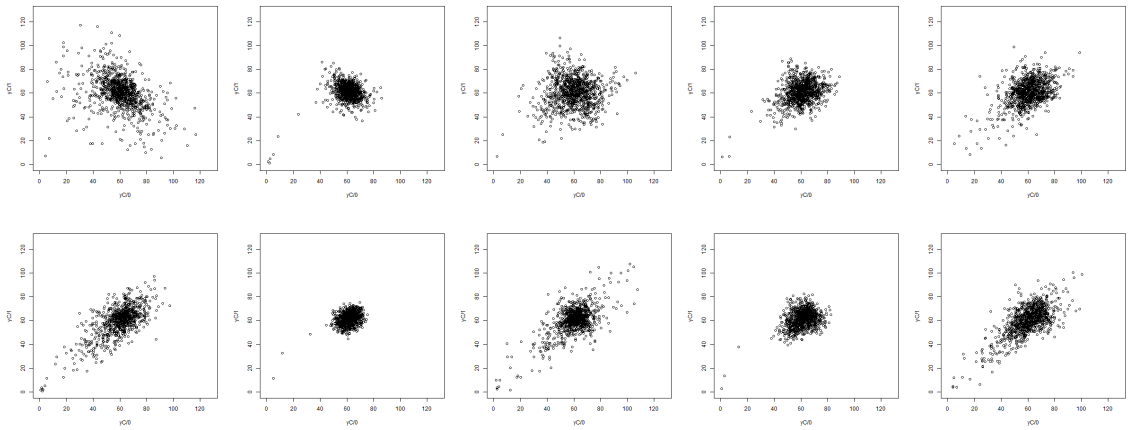

Figure 5: Phase trajectories for Y with a frequency rate from 10 Hz to 100 Hz

horizontal component and that of chaotic and regular stable quasi-stationary modes for the vertical component.

2.3 Variation of the linear beam dimension

On a number of occasions, the linear dimension of the beam can be a controlled parameter, just like the beam arriving angle. Used in the experiment targeting and focusing Gaussian wave beam allows to perform the similar transformation. It rearranges the positions of the lens group accurate within the wavelength of the radiation used [12]. Near the strangulation points of a wave beam in the observation plane it is possible to form the spots of different sizes. They can be both smaller then the size of the receiver or completely overlap its surface.

Spot sizes manipulation is reasonable under the conditions of relatively weak turbulence. The refractive diffusion in this case is relatively small. For the broadened beams propagating though an extended path even in a quiet atmosphere in their cross section there arises a local speckle structure generated by the stochastic distortions of the wave front [1]. Such a process can be observed in the two images

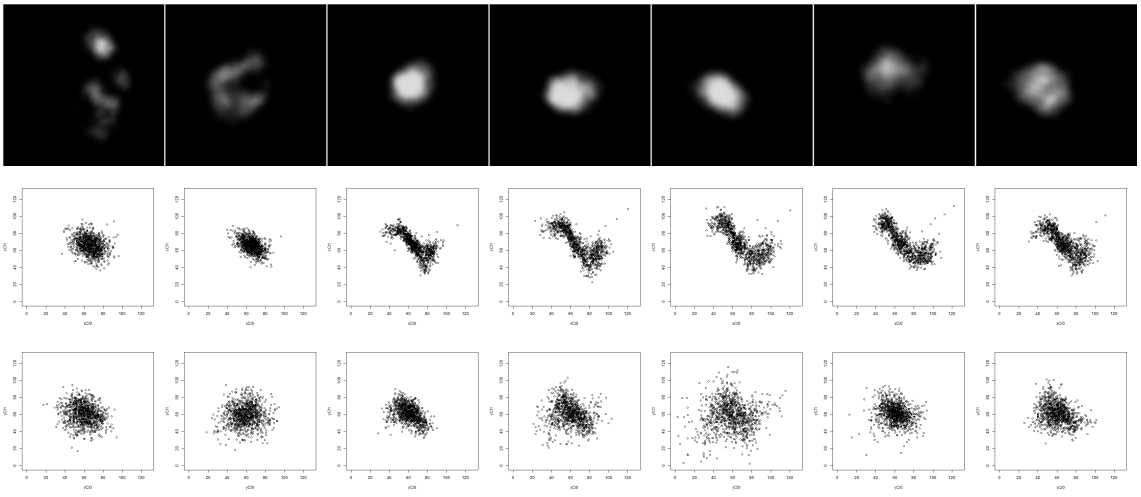

Figure 6: Video frames for the beams of different sizes (upper), phase portraits for the horizontal and vertical components of the beam center displacements (middle and bottom)

of the instantaneous intensity distributions shown in Fig.6 (left upper). Under the conditions of industrial interference the regular distortions of a characteristic spectrum in the range of low acoustic frequencies are often added. In this situation, it is reasonable to supplement the primary adaptive corrector with a frequency-selective stage, that cutting out the regular noise.

3 Geometry of the beam position detectors

The experimental results presented in the second part were obtained as an approximation of an "ideal" multichannel sensor that fixes the matrix of values of the instantaneous intensity distribution and transfers to the adaptive process the value of the beam center shift with a negligible time lag (not more than 1 millisecond). In reality one is not allowed to take the values from the entire operating field of the radiation detector. The most common options are those of the quadrant and peripheral or petal-shaped detectors. The number of parallel operating channels is limited by the decision time and the throughput of the feedback channel. In the experiment two geometric types of sensor position were tested, - a centered quadrant detector of various apertures and an eight-petaled peripheral detector with different spacing of a given petals size.
Let us define the quantitative evaluation of the time series correlations for coordinate and detector sweeps as the normalized values of the scalar multiplication of the corresponding sequences:

$$Corr_{X,Y}(\vec{D}\vec{R}) = \frac{\sum_{k=1}^{k=K} D_k R_k}{\sqrt{\left(\sum_{k=1}^{k=K} D_k^2\right)\left(\sum_{k=1}^{k=K} R_k^2\right)}} \tag{5}$$

here $\vec{D}, \vec{R}$ are the sequences of X or Y readings of the detector or the location of the

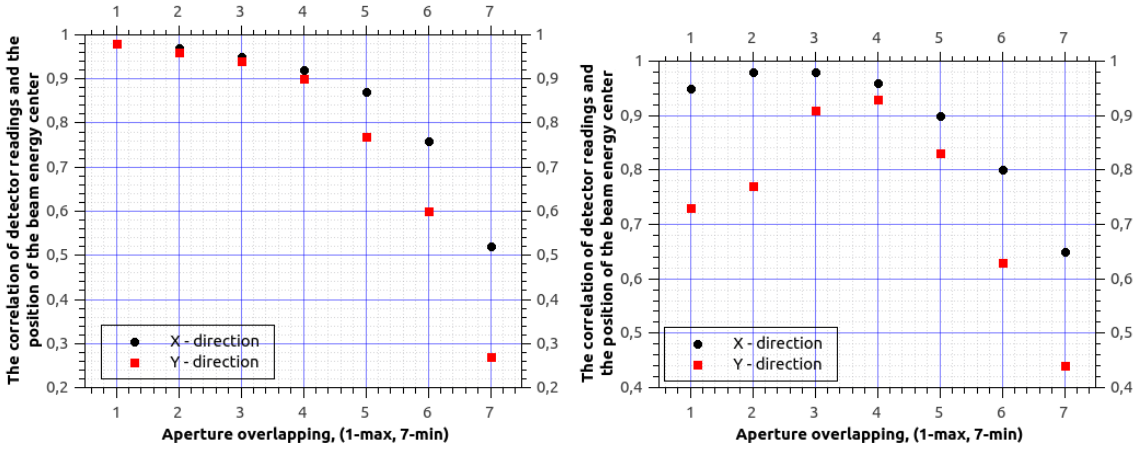

Figure 7: Correlation of the quadrant detector readings (left), the peripheral 8-lobe detector readings (right) and the position of the beam energy center for time sweeps

beam energy center. The length of the sequence corresponds to the video sample duration. The correlation value depends on the degree of the beam profile distortion, the beam splitting into fragments, absorption and scattering at the path. The typical dependencies of the detectors readings correlation on the size of the quadrant (for the quadrant detector) and the separation of the 10ptx10pt petal-sensors for the petal one are shown in Fig.7. The basic properties of the correlation characteristics for detectors of different geometries are retained in various realizations of the beam. Notably:

- a difference of the correlation value for the vertical and horizontal components of the beam displacements from the center of the operating platform,
- the existence of an optimal radius of the petals separation from the center for a particular turbulent state of the atmospheric path.

The adaptive correction process of the beam center position was compared for the quadrant and peripheral geometry of the sensor layout and the results are presented in Fig.8. The first and the third rows show the beam state sequences at the registration plane (a sampling rate is equal to 30 Hz, that corresponds to the sampling rate of the adaptive algorithm). The first and the second columns of the phase portraits correspond to the horizontal and vertical components of the center of the beam displacement, the third and the fourth columns depict the similar displacements for the proportional adapter (the readings of a square detector), the fifth and the sixth columns represent the results got for the eight-petaled peripheral detector.
As it is shown by comparative analysis of the adaptive corrector work under different sensor geometry in a wide range of the scale correction factor S, the sample intervals Δ and at various spot sizes, the peripheral detection has a low failure threshold in the cases of self-oscillatory and chaotic modes. The dispersion of the distribution function for the coordinates of the beam center in the case of quadrant positioning is much less, then that for the peripheral positioning. However, the peripheral detection practically exclude the static displacement of the beam center in a wide range of the adaptive corrector settings.

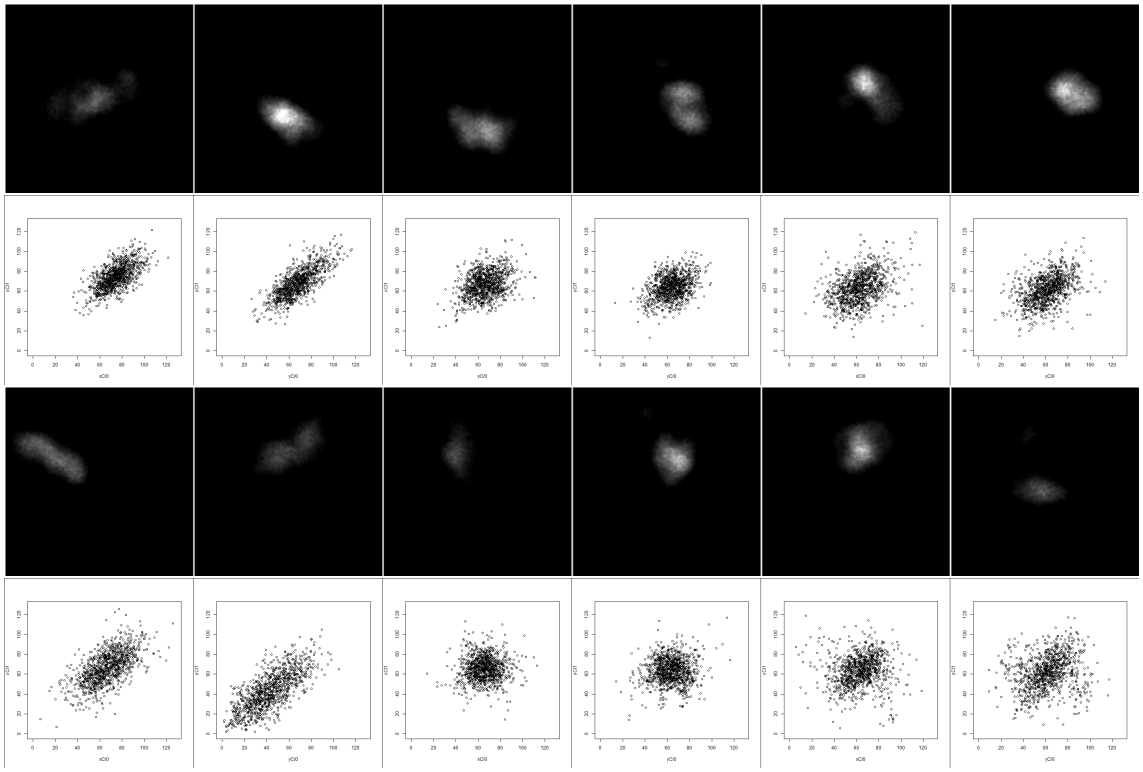

Figure 8: Examples of video frames sequences (the first and the third rows) and corresponding to them phase portraits (the second and the fourth rows)

Conclusion

The experimental study of the adaptive correction process for the first spatial moments of the beam intensity distribution at the output of a long atmospheric path was carried out. The results allow to formulate a number of statements about the stochastic and dynamic properties of the process:

- The dynamics and statistics of refraction distortions for the horizontal and vertical directions are significantly different. Accordingly the settings of the adaptive correction algorithms for orthogonal directions must be different.

- The scanning of the sampling rate for beam position detectors and the corrective procedures accomplishment reveals multiple changes of the beam movement modes for the beam center (localized near the center of the recorder, self-oscillatory, or stochastic one). They are related to the structure of the low-frequency component of the beam spot spectrum displacements in the range up to 100 Hz,

- Regular and spontaneous changes of the size of the registered beam spot under the influence of atmospheric refractive noise lead to changes in the modes of the beam center motion.

Acknowledgements

The work was supported by Russian Foundation for Basic Research. RFBR Project a-15-08-07484.

References

[1] Klyatskin V. I, *A statistical analysis of the coherent phenomena in stochastic dynamic systems*, Editorial of URSS, Moscow 2015.

[2] ArnolKєd V. I., *Geometrical methods in the theory of ordinary differential equations*, Vol. 250, Springer Science and Business Media, 2012.

[3] Takens F., "Detecting Strange Attractors in Turbulence," *Lecture Notes in Math*, Vol. 898, Springer, New York, 1981.

[4] Kennel B., Brown R., Abarbanel H.D.I., "Determining embedding dimension for phase-space reconstruction using a geometrical constructions," *Phys. Rev. A* , Vol. 45, 3403, 1992.

[5] Hong-Guang, M. A., H. A. N. Chong-zhao, "Selection of Embedding Dimension and Delay Time in Phase Space Reconstruction," *JFrontiers of Electrical and Electronic Engineering in China*, No. 1, 111–114, 2006.

[6] Kapranov V. V., Matsak I. S., Tugaenko V. Yu, Blank A. V., Suhareva N. A., "Atmospheric turbulence effects on the performance of the laser wireless power transfer system," *Proc. SPIE 10096 Free-Space Laser Communication and Atmospheric Propagation XXIX*, 100961E (February 24, 2017); doi:10.1117/12.2252013

[7] Blank A. V., Kapranov V. V., Mikhailov R. V., Suhareva N. A., Tugaenko V. Yu, "Non-linear dynamics of positional parameters of the collimated coherent beam at the end of the long atmospheric path," *Proceedings of PIERS*, 2017 (in press)

[8] Noakes L., "The Takens embedding theorem," *International Journal of Bifurcation and Chaos*, Vol. 1, No. 4, 867–972, 1991.

[9] Sauer T., J. Yorke, V. Casdagli, "Embedology," *Journal of statistical Physics*, Vol. 65, No. 3, 579–616, 1991.

[10] Shanin O. I., *Adaptive optical systems of inclinations correction. Resonance adaptive optics*, Technospera, Moscow 2013.

[11] Kapranov M. B., Tomashevsky A. I., *The regular and chaotic dynamics of nonlinear systems with discrete time*, MEI publishing house, Moscow 2009.

[12] Kapranov V. V., Matsak I. S., Tugaenko V. Yu, Blank A. V., Suhareva N. A., "Super narrow beam shaping system for remote power supply at long atmospheric path," *Proc. SPIE 10090, Laser Resonators, Microresonators, and Beam Control XIX*, 100900U (February 20, 2017); doi:10.1117/12.2250752

Arkadiy V. Blank, S.P. Korolev Rocket and Space Corporation "Energia",Russia,Moscow
M.V. Lomonosov State University, Russia
Vitaliy V. Kapranov, S.P. Korolev Rocket and Space Corporation "Energia", Russia
Ruslan V. Mikhailov, Moscow M.V. Lomonosov State University, Russia
Natalia A. Suhareva, Moscow M.V. Lomonosov State University,Russia
Vjacheslav Yu. Tugaenko, S.P. Korolev Rocket and Space Corporation "Energia", Russia